

1 **Measurement report: Nitrogen Isotope ($\delta^{15}\text{N}$) Signatures of Ammonia Emissions**
2 **from Livestock Farming: Implications for Source Apportionment of Haze**
3 **Pollution**

4 Jinhan Wang¹, Zhaojun Nie¹, Yupeng Zhang¹, Xiaolei Jie^{1,2}, Haiyang Liu¹, Peng
5 Zhao^{1,2,3}, Hongen Liu^{1,2,3}

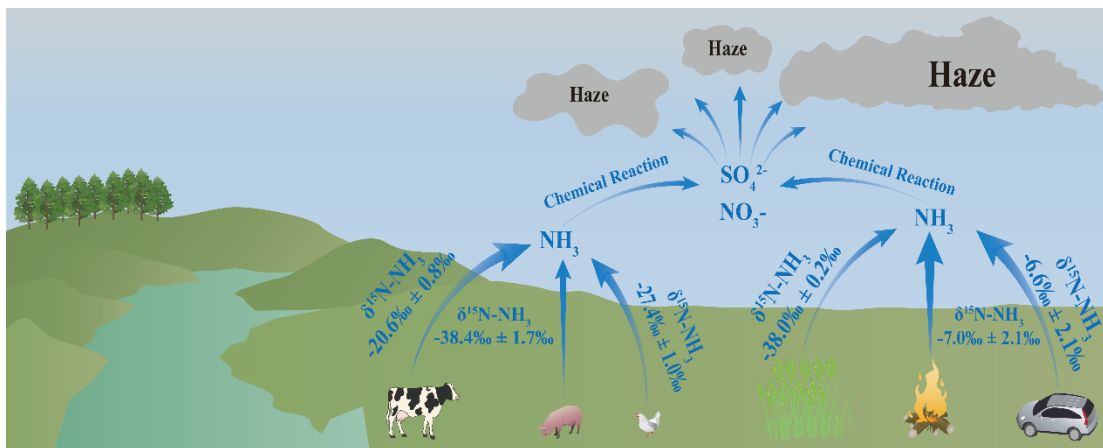
6 ¹ College of Resources and Environment, Henan Agricultural University, Zhengzhou, Henan 450046,
7 China;

8 ² Key Laboratory of Farmland Quality Conservation in the Huang-Huai-Hai Plain, Ministry of
9 Agriculture and Rural Affairs, Zhengzhou 450046, China;

10 ³ Key Laboratory of Soil Pollution Prevention, Control and Remediation in Henan Province, Zhengzhou
11 450046, China.

12 *Correspondence to:* Hongen Liu, Email: liuhongen7178@126.com; Yupeng Zhang, Email:
13 zhangyp@henau.edu.cn

14 **Abstract.** Ammonia emissions from agriculture are the primary source of atmospheric reactive nitrogen,
15 significantly impacting air pollution, soil acidification, eutrophication of water bodies, and human health.
16 Accurate quantification of ammonia from different sources is crucial for effective mitigation. In this
17 study, the air extraction method was employed to collect gases from livestock farms, and the $\delta^{15}\text{N}$ values
18 of volatilized ammonia (NH_3) from the animal husbandry industry in the southern Huang - Huai - Hai
19 Plain of China were analyzed using stable nitrogen isotopes. The results show that isotopic signatures
20 differ significantly among livestock types: dairy cows ($-20.6\text{‰} \pm 0.8\text{‰}$), laying hens ($-27.4\text{‰} \pm 1.0\text{‰}$),
21 and pigs ($-38.4\text{‰} \pm 1.7\text{‰}$). These livestock-derived signatures are distinct from those associated with
22 combustion sources ($-7.0\text{‰} \pm 2.1\text{‰}$) and traffic emissions ($6.6\text{‰} \pm 2.1\text{‰}$), and they exhibit considerably
23 lower variability than fertilizer-derived signatures. Overall, this work provides high-precision isotopic
24 source signatures for livestock operations, offering essential parameters for regional atmospheric
25 ammonia source apportionment and highlighting the need for locally tailored mitigation strategies.



26

27 Graphical Abstract.

28 1. Introduction

29 Ammonia (NH_3) is a highly reactive and abundant nitrogenous gas in the atmosphere. It is classified
 30 as a major alkaline species and readily reacts with sulfuric acid and nitric acid to produce ammonium
 31 sulfate ($(\text{NH}_4)_2\text{SO}_4$) and ammonium nitrate (NH_4NO_3) (Kawashima et al., 2023; Kirkby et al., 2011).
 32 These compounds can form particulate ammonium salts or interact with organic aerosols to generate
 33 secondary aerosols. In moderately polluted environments, the mass fraction of these ammonium-
 34 containing particles within $\text{PM}_{2.5}$ is relatively low (Huang et al., 2014; Yang et al., 2011). Under severe
 35 pollution conditions, however, ammonium sulfate, ammonium nitrate, and other ammonium salts can
 36 account for up to approximately 50% of the total $\text{PM}_{2.5}$ mass (Battye, 2003; Beusen et al., 2008; Goebes
 37 et al., 2003). As a key precursor of secondary inorganic aerosols, NH_3 is a primary contributor to haze
 38 formation and constitutes a substantial component of $\text{PM}_{2.5}$ in polluted atmospheres (Wu et al., 2024;
 39 Xiang et al., 2022). Excessive ammonia emissions also drive a range of environmental problems,
 40 including soil acidification, climate perturbation, reduced atmospheric visibility, and eutrophication of
 41 aquatic ecosystems (Huang et al., 2012; Jiang et al., 2021). Consequently, reducing NH_3 emissions has
 42 recently been proposed as a strategy to mitigate smog pollution in China (Liu et al., 2019).

43 Over the past few decades, substantial changes in air quality have been observed across many
 44 countries worldwide (Boyle, 2017; Warner et al., 2017). Notably, China has consistently ranked first in
 45 global ammonia (NH_3) emissions (Liu et al., 2013). Current NH_3 emission inventories identify the
 46 principal sources as agricultural activities-including fertilizer application and livestock and poultry
 47 farming-and non-agricultural sources, such as combustion processes and vehicular emissions (Bouwman

48 et al., 1997; Schlesinger and Hartley, 1992; Streets et al., 2003). It is widely recognized that agriculture
49 represents the predominant source of atmospheric NH₃, contributing over 70% of total emissions (Meng
50 et al., 2017; Xu et al., 2024), accounting for more than 70% of the total (Ma et al., 2021; Ti et al., 2019),
51 with livestock and poultry farming alone accounting for for 50% to 60% of agricultural NH₃ emission
52 (Huang et al., 2012; Wang et al., 2018). Despite this, substantial uncertainty remains regarding the
53 contribution of livestock-derived NH₃ to nitrogen deposition (Elliott et al., 2019), and estimating these
54 contributions using satellite remote sensing and livestock emission inventories remains challenging
55 (Beusen et al., 2008; Li et al., 2023a; Van Damme et al., 2018). These conventional approaches typically
56 rely on fixed emission factors, such as unit animal excretion coefficients, which are limited by temporal
57 lags and insufficient spatial resolution, thereby hindering the capture of real-time variations in NH₃
58 emissions and the resulting nitrogen deposition at the farm scale. In contrast, nitrogen stable isotope
59 analysis ($\delta^{15}\text{N}$) provides a direct and highly effective approach for tracing the sources of NH₃ and NH₄⁺
60 (Bhattarai et al., 2020; Xiao et al., 2020). This methodology relies on the principle that distinct emission
61 sources and environmental processes generally exhibit unique isotopic fingerprints (Elliott et al., 2019;
62 Li et al., 2024; Sui et al., 2020), defined by the ratio of heavy (¹⁵N) to light (¹⁴N) nitrogen isotopes in
63 collected samples (Song et al., 2021).

64 Numerous studies have employed stable nitrogen isotope ($\delta^{15}\text{N}$) techniques to quantify the
65 contributions of combustion, transportation, and agricultural activities to atmospheric NH₃ and NH₄⁺
66 (Xiang et al., 2022; Xie et al., 2008). For example, during the corn growing season in Northeast China,
67 $\delta^{15}\text{N}$ values of NH₃ volatilized from farmland exhibited a wide range, from -38.0‰ to -0.2‰. Notably,
68 $\delta^{15}\text{N}$ emission rates were considerably lower during the early stages of corn growth compared to later
69 stages, indicating clear seasonal variation (Song et al., 2024). Under different fertilization regimes,
70 significant differences in $\delta^{15}\text{N}$ -NH₃ emissions were observed, with values fluctuating between -46.0‰
71 and -4.7‰ throughout the volatilization period (Ti et al., 2021). Previous studies report that $\delta^{15}\text{N}$ -NH₃
72 and $\delta^{15}\text{N}$ -NH₄⁺ emissions from combustion sources (-7.6‰ to +16.2‰) predominate in winter,
73 contributing up to 51.6% of total ammonia emissions (Xiao et al., 2022, 2025; Zhou et al., 2021). In
74 contrast, NH₃ emissions from vehicle exhaust exhibit relatively high $\delta^{15}\text{N}$ values ($13.7 \pm 3.7\text{‰}$) (Savard
75 et al., 2017; Xi et al., 2023). However, these emissions are primarily localized in urban environments.

76 Currently, limited studies have reported the $\delta^{15}\text{N}$ characteristics of ammonia from livestock and
77 poultry farming. Existing data mostly rely on passive sampling methods (Berner and David Felix, 2020;

78 Chang et al., 2016; Ti et al., 2018), which assess $\delta^{15}\text{N}$ changes by collecting wet deposition samples
79 surrounding farms (pig farms: -35.1‰ to -10.5‰; cattle farms: -24.7‰ to -11.3‰). Additional research
80 has quantified $\delta^{15}\text{N}$ variability in livestock and poultry (-31.0‰ to -15.0‰) through simulated ammonia
81 emissions during manure management processes (Hristov et al., 2009). It is noteworthy that $\delta^{15}\text{N-NH}_3$
82 fluctuations in livestock and poultry operations may also depend on animal growth stages and
83 reproductive status..

84 The MixSAIR model has primarily been employed to apportion the contributions of atmospheric
85 emission sources using isotope analysis (Chang et al., 2016; Walters et al., 2022). However, there is no
86 universally fixed $\delta^{15}\text{N-NH}_4^+$ value for each emission source. As a result, substantial variations in reported
87 $\delta^{15}\text{N-NH}_4^+$ values for the same source have been documented across different studies. To date, no
88 research has validated changes in $\delta^{15}\text{N-NH}_4^+$ resulting specifically from livestock and poultry farm
89 emissions, nor has the relationship between $\delta^{15}\text{N-NH}_4^+$ from different sources and regional variations
90 been examined. To obtain more accurate assessments of $\delta^{15}\text{N-NH}_3$ variations associated with ammonia
91 emissions from livestock and poultry farming, and to achieve reliable atmospheric NH_3 source
92 apportionment, it is essential to characterize the correlation between $\delta^{15}\text{N-NH}_4^+$ from different sources
93 and regional differences. In this study, active dynamic sampling methods were used to collect ammonia
94 emissions from intensive pig farms, dairy farms, and laying hen farms located in the southern region of
95 the Huang-Huai-Hai Plain. Meta-analysis techniques were employed to analyze the $\delta^{15}\text{N}$ signatures of
96 different ammonia emission sources. The specific objectives of this research are: (1) to determine the
97 $\delta^{15}\text{N-NH}_4^+$ values of emissions from livestock and poultry housing at various growth stages; and (2) to
98 investigate the relationship between $\delta^{15}\text{N-NH}_4^+$ from different sources and regional variations.

99 **2. Materials and methods**

100 **2.1. Sampling points in the study area and sample collection and processing.**

101 The sampling experiment at the farm was conducted from May 9, 2024, to December 6, 2024. No
102 samples were collected in July and August due to the absence of livestock or poultry during these months.
103 The collected samples covered the entire breeding period of fattening pigs and the period from chicks to
104 peak egg production in laying hens. Throughout the trial period, six batches of samples were obtained,
105 amounting to a total of 120 samples for measuring ammonia emissions from livestock and poultry

106 housing. On days when samples were collected during hazy weather, the air pollution level was classified
107 as severe, whereas samples collected under clean atmospheric conditions corresponded to air quality
108 classified as excellent. Samples were collected using atmospheric samplers (Beijing Ke'an Labor
109 Protection Company) at a flow rate of 0.1 to 2 L·min⁻¹, with each sample collected over a duration of 60
110 minutes.

111 The intensive fattening pig farm is located in Luoyang City, Henan Province (112.71° E, 34.52° N),
112 with no other livestock operations in the surrounding area. The sampled fattening pig farm houses 2,600
113 pigs distributed across four fully enclosed pig houses. One of these houses was selected as the target
114 sampling site. The sampling procedure was as follows: an atmospheric sampler was positioned 2.0 meters
115 from the exhaust vent of the livestock and poultry house at a height of 1.6 meters, corresponding to the
116 central height of the exhaust outlet. The sampling duration was set to 60 minutes, with the gas flow
117 rate maintained at 2 L·min⁻¹ using a flow meter. A bubbler absorption bottle filled with absorption
118 solution was used to collect NH₃. Three atmospheric samplers were operated simultaneously during each
119 sampling event. Figure 1 marks the sampling points of the intensive pig farms with green pentagrams.

120 In the case of intensive laying hens farms, each building houses approximately 15,000 laying hens
121 and is fully enclosed, with a total of 300,000 laying hens being raised. The sampling site is located in
122 Zhengzhou City, Henan Province (114.03° E, 34.59° N). One building was selected as the target sampling
123 point, with the sampling method mirroring that used for the fattening pig farms. As shown in Figure 1,
124 the light blue pentagons represent the sampling points of intensive layer farms.

125 The intensive dairy farm operates with an open-style barn design, housing 400 dairy cows per barn,
126 with a total of 4,000 dairy cows being raised. Four atmospheric samplers were installed in the
127 passageways of the dairy barns, with each sampler spaced 10 meters apart and positioned at a height of
128 1.6 meters. The dairy farm is located in Zhengzhou City, Henan Province (114.11° E, 34.81° N). The
129 sampling time and method remained consistent with those described above. In Figure 1, the dark blue
130 pentagons represent the sampling points of intensive dairy farms.

131 To investigate the variations in $\delta^{15}\text{N}$ levels associated with differing degrees of air pollution, samples
132 collected for $\delta^{15}\text{N}$ measurement during periods of severe smog and when air quality was pristine. The
133 sampling location was situated on a spacious lawn within the campus of Henan Agricultural University,
134 devoid of tall buildings or traffic. The sampling point is illustrated in Figure 1, where the pink triangle
135 represents the sampling site for both haze and clean air (Longitude 113.82° E, Latitude 34.80° N). Each

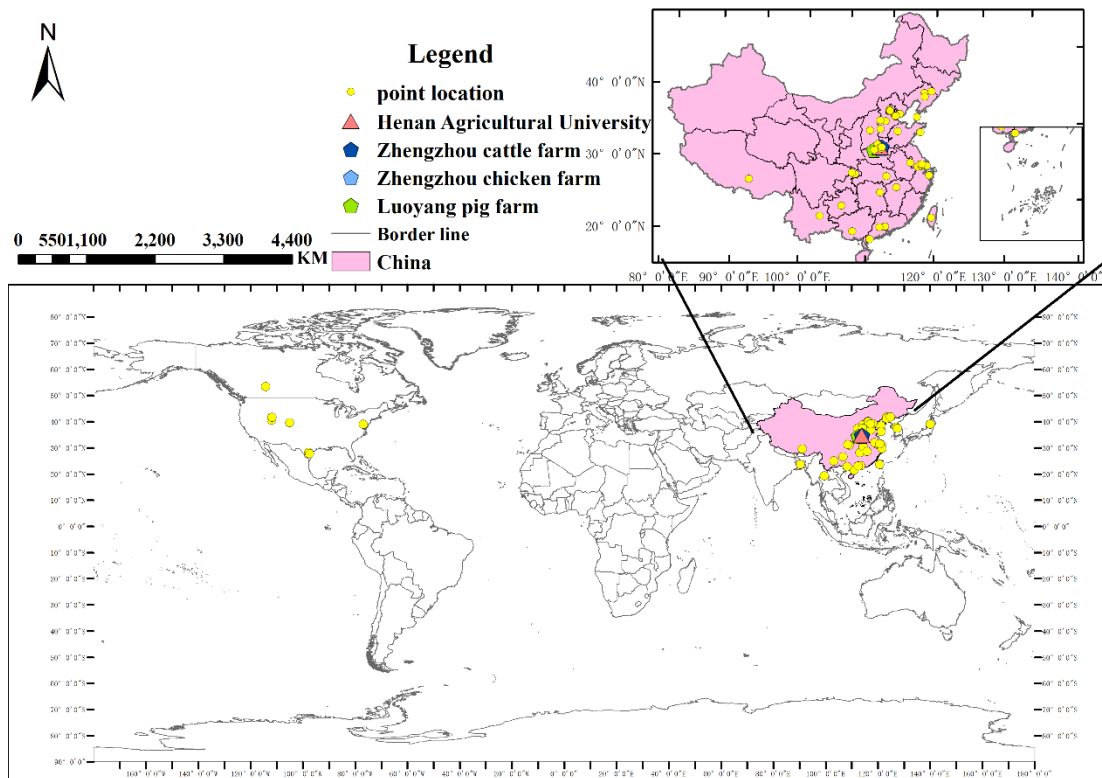
136 sampling event utilized three atmospheric samplers, positioned at a height of 1.6 meters, with the duration
137 of sampling aligned with that of the livestock farm.

138 The collected sample solution is transferred into a centrifuge tube and returned to the laboratory,
139 where the concentration of NH₃ is measured using a UV spectrophotometer. The detection method
140 adheres to the guidelines outlined in “Determination of Ammonia Nitrogen in Water by Salicylic Acid
141 Spectrophotometry” (HJ 536-2009), and the calculation method is presented in Equation (1):

$$142 \quad \rho_N = \frac{A_s - A_b - a}{b \times V} \times D \quad (1)$$

143 Where, ρ_N represents the mass concentration of ammonia nitrogen in the water sample (expressed as N),
144 in mg·L⁻³. The variables are defined as follows: A_s denotes the absorbance of the sample, while A_b
145 indicates the absorbance of the blank experiment, which is prepared from the same batch as the sample.
146 The parameters a and b correspond to the intercept and slope of the calibration curve, respectively.
147 Additionally, V refers to the volume of the water sample taken, measured in mL, and D signifies the
148 dilution factor of the water sample.

149 The analytical method described employs the bromate-hydroxylamine chemical approach (Soler-
150 Jofra et al., 2016; Zhang et al., 2007). Initially, a potassium bromate-potassium bromide solution reacts
151 under acidic conditions to produce bromine, which subsequently reacts in a strongly alkaline
152 environment to generate bromate, a potent oxidizing agent capable of oxidizing NH₄⁺ to NO₂⁻. In the
153 following step, hydroxylamine hydrochloride reduces NO₂⁻ in an acidic environment to form N₂O. The
154 resultant N₂O is then analyzed using a stable isotope ratio mass spectrometer, along with a multi-purpose
155 online gas preparation device, and an automatic sampler, to determine the $\delta^{15}\text{N}$ value. For each sample
156 analysis, four international standard materials for NH₄⁺ (IAEA-N-1, USGS-25, IAEA-N-2, and USGS-
157 26, with $\delta^{15}\text{N}$ concentrations of 0.4‰, -30.41‰, 20.3‰, and 53.75‰, respectively) are processed
158 simultaneously.



159

160 Figure 1. Sampling sites of livestock farms, haze weather, and clear weather in this study, extracted from
 161 the main research sampling locations. Yellow dots represent the main global research sampling sites, pink
 162 triangles represent sampling sites during haze and clear weather, dark blue pentagons represent cattle
 163 farms, light blue pentagons represent layer farms, and green pentagons represent fattening pig farms.

164 **2.2. Data collection and processing**

165 We screened articles published between January 2000 and January 2025 regarding the sources of
 166 $\delta^{15}\text{N-NH}_3$ and $\delta^{15}\text{N-NH}_4^+$. Specifically, we utilized ISI Web of Science, Google Scholar, and PubMed,
 167 employing the search terms “ $\delta^{15}\text{N}$,” “ NH_3 ,” “ammonia emissions,” and “isotopes” to identify relevant
 168 literature. Studies included in our analysis were required to meet the following criteria: (1) Samples must
 169 be measured for either $\delta^{15}\text{N-NH}_3$ or $\delta^{15}\text{N-NH}_4^+$; (2) Experiments must encompass at least one of the
 170 following: combustion, fertilization, agriculture, transportation, or livestock farming; (3) The number of
 171 experimental replicates and sampling events must be explicitly reported; (4) Samples must primarily
 172 consist of atmospheric NH_3 or $\text{PM}_{2.5}$, and detection must employ chemical methods. A total of 37
 173 documents were included in the analysis. This dataset comprehensively encompasses multiple meta-
 174 analyses and original studies, detailing changes in $\delta^{15}\text{N-NH}_3$ and $\delta^{15}\text{N-NH}_4^+$ from combustion sources,
 175 transportation sources, agricultural sources, and livestock farming sources; the proportion of $\delta^{15}\text{N}$ values

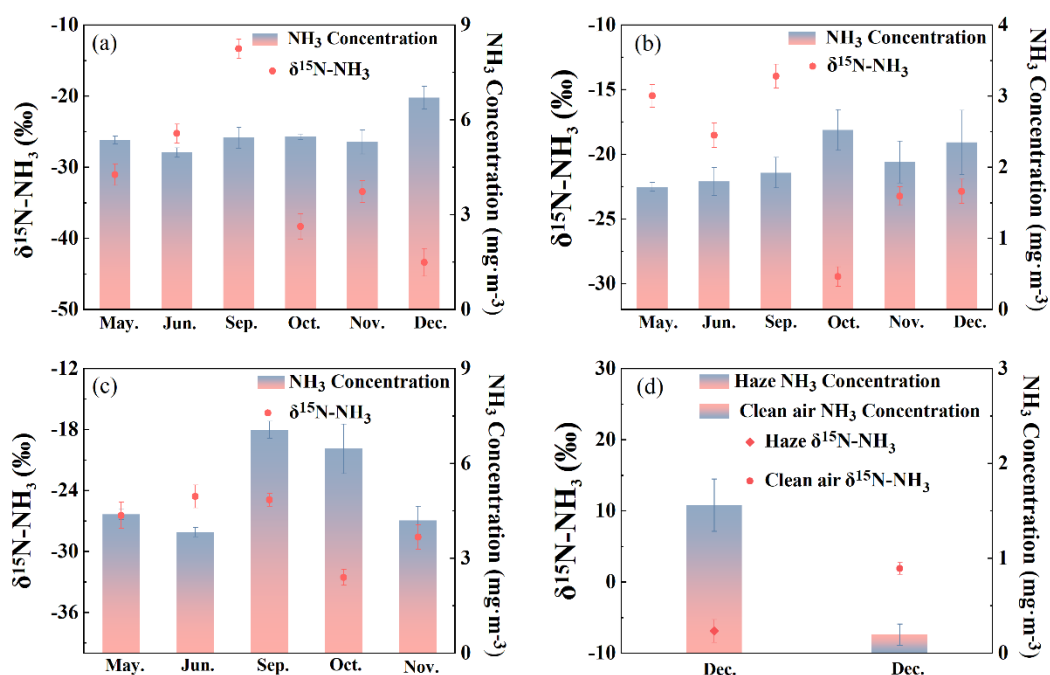
176 in the atmosphere; geographical location (latitude and longitude); and the GDP of each city where
177 samples were collected. If the data in the literature was presented solely in chart form, we utilized
178 WebPlotDigitizer-4.7 (<https://apps.automeris.io/wpd4/>) to extract the data. We categorized the collected
179 data into five distinct groups: combustion, transportation, farmland, livestock farming, and PM_{2.5}.

180 A total of 126 samples were collected, and 41 literature references were gathered. Data analysis was
181 performed using Excel, SPSS, and Python version 3.11.

182 3. Result and discussion

183 3.1. Temporal Variations in Ammonia Emissions and $\delta^{15}\text{N}$ Signatures from Livestock Farms

184 During the sampling period from May to December, ammonia emissions varied significantly among
185 the three farm types: 4.9 to 6.7 mg·m⁻³ for fattening pigs (Figure 2a), 1.7 and 2.5 mg·m⁻³ for dairy cows
186 (Figure 2b), and 3.8 to 7.1 mg·m⁻³ for laying hens (Figure 2c), with the latter exhibiting substantial
187 temporal fluctuations. NH₃ emissions from fattening pigs peaked when the pigs reached 130 kg·head⁻¹
188 (Figure 2a), For laying hens, NH₃ concentrations initially increased and subsequently declined in
189 response to temperature variations, reflecting enhanced urease activity within the housing environment,
190 which accelerates urea hydrolysis and promotes NH₃ volatilization. $\delta^{15}\text{N-NH}_4^+$ levels at the livestock
191 farms showed significant temporal variation ($p < 0.05$) (Groot Koerkamp et al., 1998; Rosa et al., 2020).
192 From May to June, the $\delta^{15}\text{N-NH}_4^+$ From May to June, $\delta^{15}\text{N-NH}_4^+$ increased from -31.0‰ to -25.2‰ in
193 fattening pig farms and from -26.4‰ to -24.6‰ in laying hen farms. In September, $\delta^{15}\text{N-NH}_4^+$ values
194 from fattening pig farms ($-13.3 \pm 1.3\%$) were significantly higher than those from laying hen and dairy
195 cow farms ($-13.9 \pm 0.9\%$), which were comparable. Over the following three months, $\delta^{15}\text{N-NH}_4^+$ levels
196 decreased significantly across both farm types. As illustrated in Figure 2, the highest NH₃ concentration
197 at the dairy farm ($2.5 \pm 0.3 \text{ mg}\cdot\text{m}^{-3}$) occurred in October, coinciding with the lowest $\delta^{15}\text{N-NH}_4^+$ values.
198 while laying hen farms also recorded minimum $\delta^{15}\text{N-NH}_4^+$ during this period of elevated NH₃.
199 Conversely, the lowest $\delta^{15}\text{N-NH}_4^+$ at fattening pig farms was observed in December, despite peak NH₃
200 concentrations. NH₃ concentrations differed significantly between hazy and clear weather in December
201 (Figure 2d), with $\delta^{15}\text{N-NH}_4^+$ values being significantly higher under clear conditions ($1.9 \pm 0.8\%$) than
202 under hazy conditions ($1.6 \pm 0.2\%$; $p < 0.05$).

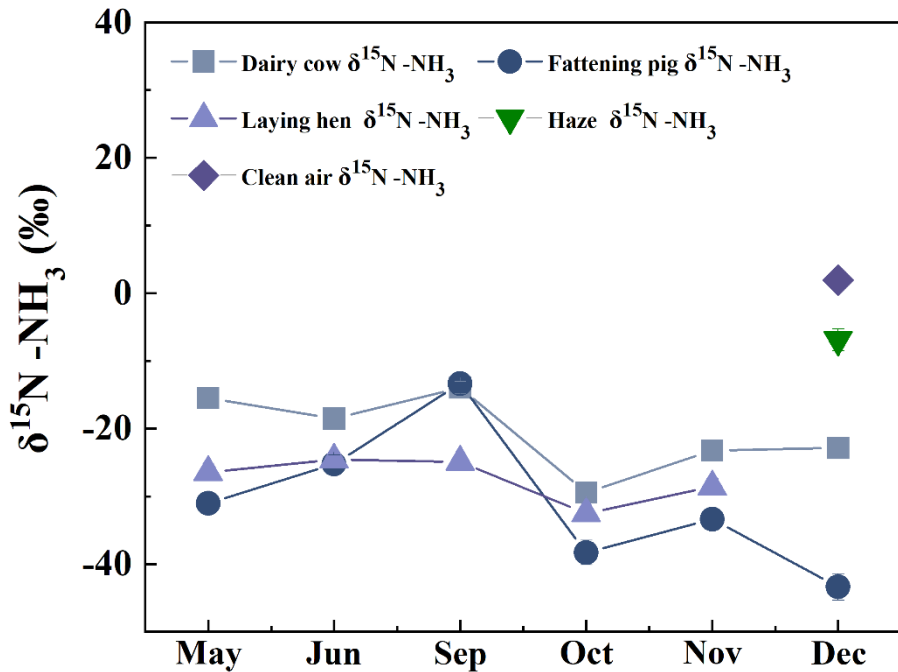


203

204 Figure 2. Changes in NH₃ emissions and $\delta^{15}\text{N-NH}_4^+$ values outside the livestock farms among different
 205 months. (a)Fattening pig farm; (b)Dairy cow farm; (c) Laying hens farm; (d) Comparison of Haze and clean
 206 air samples. Statistical difference was calculated by T-test, $P < 0.05$, $n = 3$.

207

As illustrated in Figure 3, throughout the entire monitoring period, ammonia (NH₃) sources from
 208 the farms exhibited nitrogen depletion, indicated by negative $\delta^{15}\text{N-NH}_4^+$ values. Overall, $\delta^{15}\text{N-NH}_4^+$
 209 values exhibited significant fluctuations in dairy and fattening pig farms, while variations were
 210 comparatively moderate in laying hens farms. Notably, the $\delta^{15}\text{N-NH}_4^+$ values at dairy cattle farms
 211 displayed substantially greater overall changes during the monitoring period compared to those in laying
 212 hens and fattening pig farms. The arithmetic mean value at fattening pig farms was $-30.8 \pm 1.6\%$, the
 213 lowest among the three types of farms, whereas the $\delta^{15}\text{N-NH}_4^+$ values in laying hens manure remained
 214 at an intermediate level throughout the entire period. From October to December, the $\delta^{15}\text{N-NH}_4^+$ values
 215 at livestock and poultry farms were generally lower than those observed in the first half of the monitoring
 216 period (Figure 3). However, when comparing hazy and clear weather conditions, the $\delta^{15}\text{N-NH}_4^+$ values
 217 for all three types of farms consistently remained at a relatively low level during this timeframe (Figure
 218 3).



219

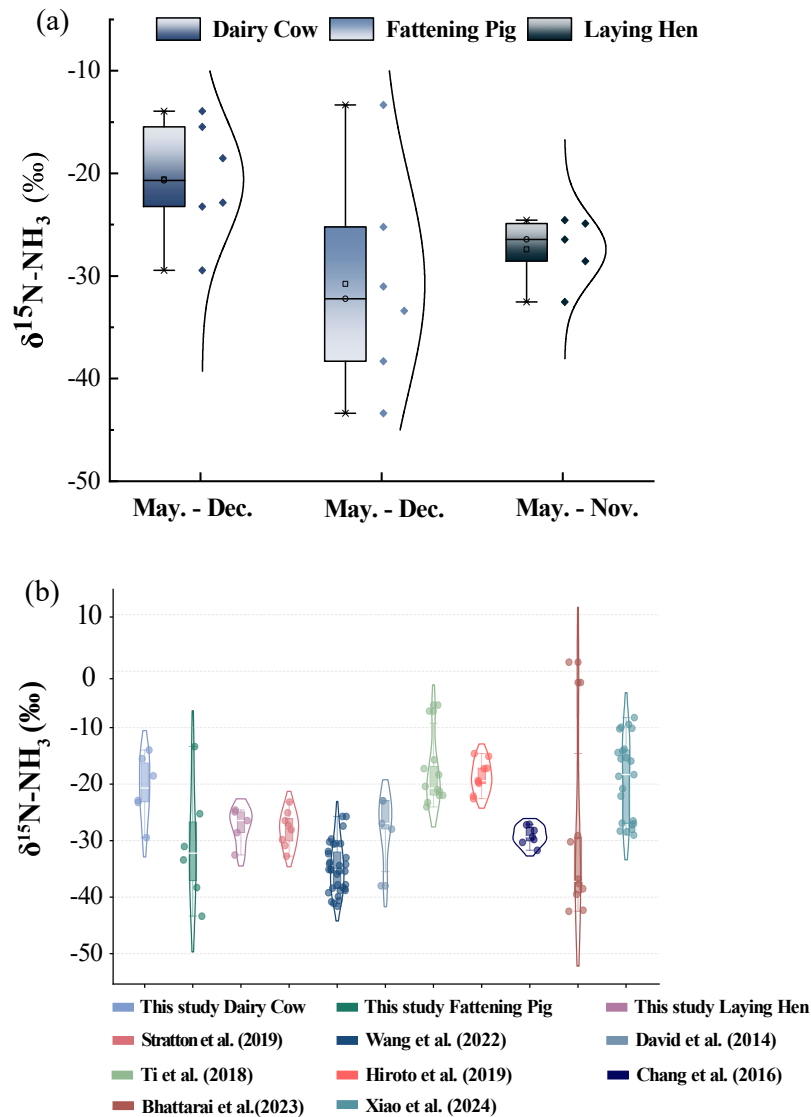
220 Figure 3. Changes of $\delta^{15}\text{N-NH}_4^+$ abundance at intensive livestock farms during the sampling period. Hazy
 221 and clean air were also sampled at December. The air sample of laying hens in December was missed,
 222 because of death of chicken by avian influenza.

223 3.2. Comparison with Literature and Implications for Local Sources

224 During the monitoring period, the $\delta^{15}\text{N-NH}_4^+$ values ranged from -50.0‰ to -10.0‰ (Figure 4a).
 225 For fattening pigs, $\delta^{15}\text{N-NH}_4^+$ values averaged -38.4‰ \pm 1.8‰ between October and December, which
 226 was significantly lower than the previously reported range of -27.10‰ to -31.7‰ (Chang et al., 2016)
 227 Notably, the overall variation remained within the $\delta^{15}\text{N-NH}_4^+$ emission ranges report for fattening pigs
 228 in other studies (Bhattarai and Wang, 2023; Wang et al., 2022). Furthermore, due to differences in
 229 livestock management practices and nitrogen content in feed, the $\delta^{15}\text{N-NH}_4^+$ values from dairy farms in
 230 this study, averaging -29.4‰ \pm 13.9‰, were substantially lower than those reported by Martine M et al.
 231 (20.5‰ \pm 34.5‰) (Savard et al., 2017).

232 Comparison with $\delta^{15}\text{N-NH}_4^+$ values measured in dairy farms in Akita, Japan, were -22.5‰ \pm -14.6‰
 233 (Kawashima, 2019), no significant difference was observed relative to the values obtained in this study.
 234 However, these values exceeded those reported by David et al (Felix et al., 2014), which ranged from -

235 37.9‰ to -22.9‰ based on passive sampling techniques. Previous research has shown that active
236 sampling generally yields higher $\delta^{15}\text{N}$ values than passive sampling (Kawashima and Ono, 2019; Pan et
237 al., 2020). This discrepancy arises from the diffusion-driven nature of passive samplers, in which lighter
238 NH_3 molecules are preferentially adsorbed. Consequently, passive sampling typically produces $\delta^{15}\text{N}$
239 values that deviate by approximately 15‰ from those obtained by active sampling (Bhattarai and Wang,
240 2023; Skinner et al., 2006). Variations in $\delta^{15}\text{N-NH}_4^+$ values are known to occur among different livestock
241 species. During the monitoring period, $\delta^{15}\text{N-NH}_4^+$ values from laying hen farms were consistently lower
242 than those from dairy farms but higher than those from fattening pig farms, consistent with previously
243 reported trends. This pattern suggests that $\delta^{15}\text{N-NH}_4^+$ variations in emitted NH_3 are not primarily driven
244 by animal body weight but are instead strongly modulated by environmental conditions (Choi et al., 2017;
245 Qu and Zhang, 2021). In agreement with earlier studies, $\delta^{15}\text{N-NH}_4^+$ emissions from fattening pig and
246 laying hen farms differed significantly from previously documented values, whereas no significant
247 difference was observed for dairy cattle farms. Furthermore, the magnitude of $\delta^{15}\text{N-NH}_4^+$ fluctuations
248 across the three farm types was smaller than that reported in earlier literature. Comparison with major
249 atmospheric NH_3 sources further demonstrated that the $\delta^{15}\text{N-NH}_4^+$ values measured in this study diverged
250 substantially from those associated with combustion ($-7.0\text{‰} \pm 2.1\text{‰}$), fertilization application (-38.0‰
251 $\pm 0.2\text{‰}$), and transportation ($6.6\text{‰} \pm 2.1\text{‰}$). Based on $\delta^{15}\text{N-NH}_4^+$ signatures measured under both hazy
252 and clear weather conditions, it can therefore be inferred that agricultural and livestock emissions are not
253 the dominant contributors to atmospheric NH_3 in Zhengzhou. Instead, traffic exhaust and combustion
254 sources appear to constitute the primary contributors.



255

256 Figure 4. Comparison of $\delta^{15}\text{N-NH}_4^+$ values within different livestock farms and historical reported data.

257 (a)Comparison of the $\delta^{15}\text{N-NH}_4^+$ values among different livestock farms; (b)Comparison of the $\delta^{15}\text{N-NH}_4^+$

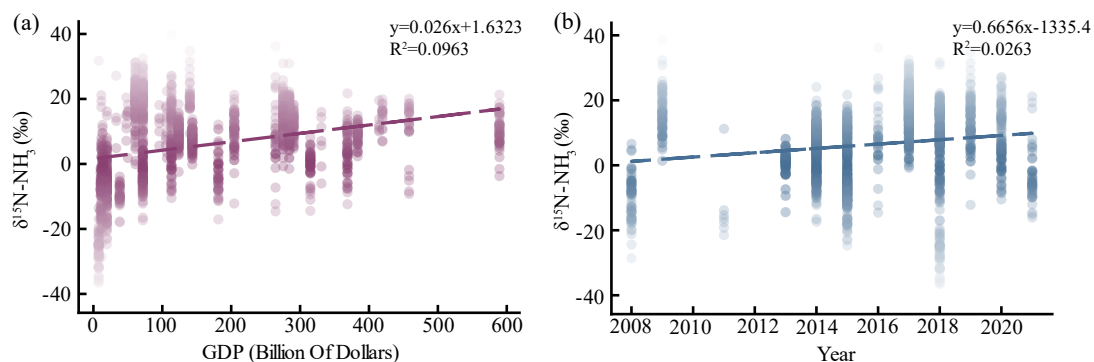
258 NH_4^+ values from present study with previously reported data.

259 3.3. Global Variability of NH_3 Source Signatures and Challenges for Source Apportionment

260 Ammonia emissions that contribute to urban smog primarily arise from combustion activities,
 261 vehicle exhaust, agriculture fertilization, and livestock production. As national economies expand, the
 262 frequency and severity of smog events have intensified. Figure 5a (slope: 0.026, intercept: 1.6323, R^2 :

263 0.0963) shows that from 2000 to 2025, when GDP remains below 70 billion USD, atmospheric $\delta^{15}\text{N-NH}_3$ -
264 NH_4^+ signatures predominantly reflect fertilizer-derived emissions from agricultural regions and NH_3
265 volatilization from livestock operations (Kawashima et al., 2022; Kawashima and Kurahashi, 2011). This
266 pattern indicates that lower-income regions rely heavily on agriculture and animal husbandry as the
267 foundational components of their economies (Leng et al., 2018).

268 When GDP increases to between 80 billion and 300 billion USD, the contribution of combustion-
269 related and vehicular sources to $\delta^{15}\text{N-NH}_4^+$ becomes increasingly prominent. Notably, vehicle exhaust
270 remains the dominant contributor within this GDP interval, suggesting that transportation serves as a key
271 economic driver during mid-stage development. In densely populated and economically advanced cities,
272 rapid vehicle growth further amplifies the influence of transportation-related $\delta^{15}\text{N-NH}_4^+$ signatures (Lim
273 et al., 2022; Pan et al., 2018; Stratton et al., 2019). Throughout the entire dataset, vehicle exhaust and
274 combustion together account for nearly 70% of ammonia emissions (Wu et al., 2019). Once GDP
275 surpasses 300 billion USD, $\delta^{15}\text{N-NH}_4^+$ from combustion becomes the dominant atmospheric source,
276 while the relative contribution from vehicle exhaust begins to decline and emissions from agricultural
277 fertilization and livestock farming become negligible (Li et al., 2023b). It is important to note that
278 sampling sites in the present study were located near power plants (Lim et al., 2019; Zou et al., 2022),
279 whereas comparison data from previous studies were collected in urban cores. This spatial difference
280 further supports the conclusion that in highly developed cities, shifts in economic structure lead to
281 combustion sources emerging as the principal contributors to atmospheric NH_3 under both hazy and clear
282 meteorological conditions. As illustrated in Figure 5b, the proportion of $\delta^{15}\text{N-NH}_4^+$ attributed to
283 combustion and vehicular sources has increased over time. This temporal trend suggests that, with
284 economic growth, agricultural and livestock emissions no longer represent the dominant contributors to
285 atmospheric ammonia.

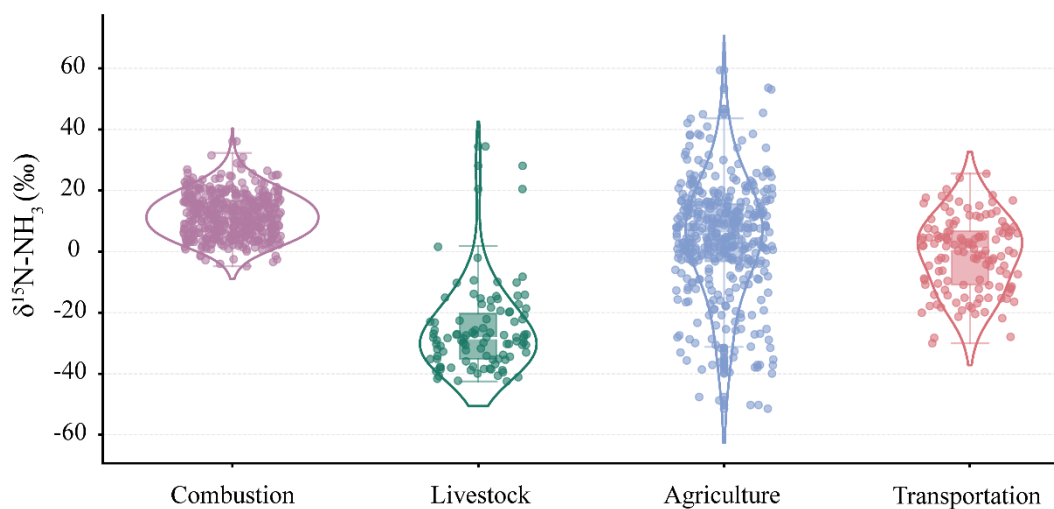


286

287 Figure 5. Changes of $\delta^{15}\text{N-NH}_4^+$ values among different GDP cities and years. (a) The relationship

288 between GDP and $\delta^{15}\text{N-NH}_4^+$ values; (b) Changes of $\delta^{15}\text{N-NH}_4^+$ values reported between 2008 to 2021.

289 The extracted dataset was classified into four major emission categories-livestock farming,
290 combustion, farmland fertilization, and vehicle exhaust-and subsequently subjected to statistical
291 evaluation. As illustrated in Figure 6, $\delta^{15}\text{N-NH}_4^+$ values associated with combustion sources showed
292 strong consistency with previously reported ranges (Chang et al., 2021). Although traffic exhaust and
293 livestock-related $\delta^{15}\text{N-NH}_4^+$ values exhibited moderate dispersion, both sources remained within
294 relatively well-defined isotopic ranges. In sharp contrast, $\delta^{15}\text{N-NH}_4^+$ signatures following farmland
295 fertilization displayed pronounced heterogeneity, covering nearly the entire isotopic spectrum reported
296 for combustion, livestock, and vehicular emissions. This extensive variability highlights substantial
297 regional differences in agricultural ammonia emission processes (Felix et al., 2014; Li et al., 2023b).
298 Consequently, accurate source apportionment of atmospheric NH_3 requires distinguishing dominant local
299 emission pathways rather than relying solely on generalized isotopic patterns (Chen et al., 2022; Zhang
300 et al., 2023).



301

302 Figure 6. Statistical analysis of extracted data categorized by source: combustion sources, livestock and
303 poultry farming sources, agricultural sources, and transportation exhaust sources.

304 4. Summary

305 This study establishes high-precision $\delta^{15}\text{N}$ signatures for ammonia emissions from three dominant
306 intensive livestock systems in the Huang-Huai-Hai Plain. Distinct isotopic fingerprints were identified

307 for dairy operations ($-20.6\% \pm 0.8\%$), laying hen facilities ($-27.4\% \pm 1.0\%$), and fattening pig farms (-
308 $38.4\% \pm 1.7\%$), underscoring clear differences among livestock categories. Our results further
309 demonstrate that isotopic signatures vary dynamically with NH_3 volatilization intensity, highlighting the
310 need to incorporate volatilization-driven fractionation effects into isotope-based source apportionment
311 frameworks. When compared with ambient $\delta^{15}\text{N-NH}_4^+$ measurements in Zhengzhou, the newly
312 constrained source end-members indicate that non-agricultural sources-particularly vehicular emissions
313 and combustion-are likely major contributors to urban atmospheric ammonia. This interpretation,
314 however, requires validation through comprehensive isotopic mixing and dispersion modeling. Moreover,
315 global-scale evaluation reveals that the exceptional variability of $\delta^{15}\text{N}$ associated with fertilized soils
316 continues to pose a substantial challenge for accurate identification of agricultural contributions.
317 Collectively, the findings presented here provide critical isotopic constraints that can enhance regional
318 atmospheric chemistry models and support the design of more precise and effective ammonia emission
319 control policies.

320 **Author Contributions**

321 J.W. Drafting, Formal Analysis, Data Management, Methodology, Investigation; Z.N. Formal Analysis,
322 Data Management, Methodology, Investigation; Y.Z. Conceptualization, Data Management,
323 Visualization, Funding Acquisition, Drafting, Formal Analysis, Writing - Review & Editing; X.J. Data
324 Management, Visualization; H.L. Data Management, Methodology; P.Z. Formal Analysis, Data
325 Management; H.L. Writing - Review & Editing, Funding Acquisition, Conceptualization, Supervision.

326 **Competing interest**

327 The authors declare that they have no known competing financial interests or personal relationships that
328 could have influenced the work reported in this paper.

329 **Acknowledgments.** This research was supported by the National Key Research and Development
330 Program of China (2021 YFD 1700900), the Industrial Technology System for Cultivated Land
331 Protection in Henan Province (HARS-22-19-S), the Natural Science Foundation of Henan Province
332 (Grant No. 252300420043), and the Key Research and Development Program of Henan Province (Grant
333 No. 251111112200).

334 **Data availability**

335 All data are available in the text, Supplement or publicly on Zenodo (DOI [10.5281/zenodo.17639507](https://doi.org/10.5281/zenodo.17639507)).

336 **References:**

337 Battye, W.: Evaluation and improvement of ammonia emissions inventories, *Atmos. Environ.*, 37, 3873–
338 3883, [https://doi.org/10.1016/S1352-2310\(03\)00343-1](https://doi.org/10.1016/S1352-2310(03)00343-1), 2003.

339 Berner, A. H. and David Felix, J.: Investigating ammonia emissions in a coastal urban airshed using
340 stable isotope techniques, *Sci. Total Environ.*, 707, 134952,
341 <https://doi.org/10.1016/j.scitotenv.2019.134952>, 2020.

342 Beusen, A. H. W., Bouwman, A. F., Heuberger, P. S. C., Van Drecht, G., and Van Der Hoek, K. W.:
343 Bottom-up uncertainty estimates of global ammonia emissions from global agricultural production
344 systems, *Atmos. Environ.*, 42, 6067–6077, <https://doi.org/10.1016/j.atmosenv.2008.03.044>, 2008.

345 Bhattarai, N. and Wang, S.: Active vs. passive isotopic analysis: insights from urban beijing field
346 measurements and ammonia source signatures, *Atmos. Environ.*, 314,
347 <https://doi.org/10.1016/j.atmosenv.2023.120079>, 2023.

348 Bhattarai, N., Wang, S., Xu, Q., Dong, Z., Chang, X., Jiang, Y., and Zheng, H.: Sources of gaseous NH₃
349 in urban beijing from parallel sampling of NH₃ and NH₄⁺, their nitrogen isotope measurement and
350 modeling, *Sci. Total Environ.*, 747, 141361, <https://doi.org/10.1016/j.scitotenv.2020.141361>, 2020.

351 Bouwman, A. F., Lee, D. S., Asman, W. a. H., Dentener, F. J., Van Der Hoek, K. W., and Olivier, J. G. J.:
352 A global high-resolution emission inventory for ammonia, *Glob. Biogeochem. Cycles*, 11, 561–587,
353 <https://doi.org/10.1029/97GB02266>, 1997.

354 Boyle, E.: Nitrogen pollution knows no bounds, *Science*, 356, 700–701,
355 <https://doi.org/10.1126/science.aan3242>, 2017.

356 Chang, Y., Liu, X., Deng, C., Dore, A. J., and Zhuang, G.: Source apportionment of atmospheric ammonia
357 before, during, and after the 2014 APEC summit in beijing using stable nitrogen isotope signatures,
358 *Atmospheric Chem. Phys.*, 16, 11635–11647, <https://doi.org/10.5194/acp-16-11635-2016>, 2016.

359 Chang, Y., Zhang, Y.-L., Kawichai, S., Wang, Q., Van Damme, M., Clarisse, L., Prapamontol, T., and
360 Lehmann, M. F.: Convergent evidence for the pervasive but limited contribution of biomass burning to
361 atmospheric ammonia in peninsular southeast Asia, *Atmospheric Chem. Phys.*, 21, 7187–7198,
362 <https://doi.org/10.5194/acp-21-7187-2021>, 2021.

363 Chen, T.-Y., Chen, C.-L., Chen, Y.-C., Chou, C. C.-K., Ren, H., and Hung, H.-M.: Source apportionment
364 and evolution of N-containing aerosols at a rural cloud forest in taiwan by isotope analysis, *Atmospheric
365 Chem. Phys.*, 22, 13001–13012, <https://doi.org/10.5194/acp-22-13001-2022>, 2022.

366 Choi, W.-J., Kwak, J.-H., Lim, S.-S., Park, H.-J., Chang, S. X., Lee, S.-M., Arshad, M. A., Yun, S.-I., and
367 Kim, H.-Y.: Synthetic fertilizer and livestock manure differently affect $\delta^{15}\text{N}$ in the agricultural landscape:
368 a review, *Agric. Ecosyst. Environ.*, 237, 1–15, <https://doi.org/10.1016/j.agee.2016.12.020>, 2017.

369 Elliott, E. M., Yu, Z., Cole, A. S., and Coughlin, J. G.: Isotopic advances in understanding reactive
370 nitrogen deposition and atmospheric processing, *Sci. Total Environ.*, 662, 393–403,
371 <https://doi.org/10.1016/j.scitotenv.2018.12.177>, 2019.

372 Felix, J. D., Elliott, E. M., Gish, T., Maghirang, R., Cambal, L., and Clougherty, J.: Examining the
373 transport of ammonia emissions across landscapes using nitrogen isotope ratios, *Atmos. Environ.*, 95,
374 563–570, <https://doi.org/10.1016/j.atmosenv.2014.06.061>, 2014.

375 Goebes, M. D., Strader, R., and Davidson, C.: An ammonia emission inventory for fertilizer application
376 in the United States, *Atmos. Environ.*, 37, 2539–2550, [https://doi.org/10.1016/S1352-2310\(03\)00129-8](https://doi.org/10.1016/S1352-2310(03)00129-8),
377 2003.

378 Groot Koerkamp, P. W. G., Metz, J. H. M., Uenk, G. H., Phillips, V. R., Holden, M. R., Sneath, R. W.,
379 Short, J. L., White, R. P. P., Hartung, J., Seedorf, J., Schröder, M., Linkert, K. H., Pedersen, S., Takai, H.,
380 Johnsen, J. O., and Wathes, C. M.: Concentrations and emissions of ammonia in livestock buildings in
381 northern Europe, *J. Agric. Eng. Res.*, 70, 79–95, <https://doi.org/10.1006/jaer.1998.0275>, 1998.

382 Hristov, A. N., Zaman, S., Vander Pol, M., Ndegwa, P., Campbell, L., and Silva, S.: Nitrogen losses from
383 dairy manure estimated through nitrogen mass balance and chemical markers, *J. Environ. Qual.*, 38,
384 2438–2448, <https://doi.org/10.2134/jeq2009.0057>, 2009.

385 Huang, R.-J., Zhang, Y., Bozzetti, C., Ho, K.-F., Cao, J.-J., Han, Y., Daellenbach, K. R., Slowik, J. G.,
386 Platt, S. M., Canonaco, F., Zotter, P., Wolf, R., Pieber, S. M., Bruns, E. A., Crippa, M., Ciarelli, G.,
387 Piazzalunga, A., Schwikowski, M., Abbaszade, G., Schnelle-Kreis, J., Zimmermann, R., An, Z., Szidat,
388 S., Baltensperger, U., Haddad, I. E., and Prévôt, A. S. H.: High secondary aerosol contribution to
389 particulate pollution during haze events in China, *Nature*, 514, 218–222,
390 <https://doi.org/10.1038/nature13774>, 2014.

391 Huang, X., Song, Y., Li, M., Li, J., Huo, Q., Cai, X., Zhu, T., Hu, M., and Zhang, H.: A high-resolution
392 ammonia emission inventory in China, *Glob. Biogeochem. Cycles*, 26,
393 <https://doi.org/10.1029/2011GB004161>, 2012.

394 Jiang, H., Zhang, Q., Liu, W., Zhang, J., Pan, K., Zhao, T., and Xu, Z.: Isotopic compositions reveal the
395 driving forces of high nitrate level in an urban river: implications for pollution control, *J. Clean. Prod.*,
396 298, 126693, <https://doi.org/10.1016/j.jclepro.2021.126693>, 2021.

397 Kawashima, H.: Seasonal trends of the stable nitrogen isotope ratio in particulate nitrogen compounds
398 and their gaseous precursors in akita, japan, *Tellus Ser. B-Chem. Phys. Meteorol.*, 71,
399 <https://doi.org/10.1080/16000889.2019.1627846>, 2019.

400 Kawashima, H. and Kurahashi, T.: Inorganic ion and nitrogen isotopic compositions of atmospheric
401 aerosols at yurihonjo, *Atmos. Environ.*, 45, 6309–6316, <https://doi.org/10.1016/j.atmosenv.2011.08.057>,
402 2011.

403 Kawashima, H. and Ono, S.: Nitrogen isotope fractionation from ammonia gas to ammonium in
404 particulate ammonium chloride, *Environ. Sci. Technol.*, 53, 10629–10635,
405 <https://doi.org/10.1021/acs.est.9b01569>, 2019.

406 Kawashima, H., Yoshida, O., Joy, K. S., Raju, R. A., Islam, K. N., Jeba, F., and Salam, A.: Sources
407 identification of ammonium in PM_{2.5} during monsoon season in Dhaka, Bangladesh, *Sci. Total Environ.*,
408 838, <https://doi.org/10.1016/j.scitotenv.2022.156433>, 2022.

409 Kawashima, H., Yoshida, O., and Suto, N.: Long-term source apportionment of ammonium in PM_{2.5} at a
410 suburban and a rural site using stable nitrogen isotopes, *Environ. Sci. Technol.*, 57, 1268–1277,
411 <https://doi.org/10.1021/acs.est.2c06311>, 2023.

412 Kirkby, J., Curtius, J., Almeida, J., Dunne, E., Duplissy, J., Ehrhart, S., Franchin, A., Gagné, S., Ickes,
413 L., Kürten, A., Kupc, A., Metzger, A., Riccobono, F., Rondo, L., Schobesberger, S., Tsagkogeorgas, G.,
414 Wimmer, D., Amorim, A., Bianchi, F., Breitenlechner, M., David, A., Dommen, J., Downard, A., Ehn,
415 M., Flagan, R. C., Haider, S., Hansel, A., Hauser, D., Jud, W., Junninen, H., Kreissl, F., Kvashin, A.,
416 Laaksonen, A., Lehtipalo, K., Lima, J., Lovejoy, E. R., Makhmutov, V., Mathot, S., Mikkilä, J.,
417 Minginette, P., Mogo, S., Nieminen, T., Onnela, A., Pereira, P., Petäjä, T., Schnitzhofer, R., Seinfeld, J.
418 H., Sipilä, M., Stozhkov, Y., Stratmann, F., Tomé, A., Vanhanen, J., Viisanen, Y., Vrtala, A., Wagner, P.
419 E., Walther, H., Weingartner, E., Wex, H., Winkler, P. M., Carslaw, K. S., Worsnop, D. R., Baltensperger,
420 U., and Kulmala, M.: Role of sulphuric acid, ammonia and galactic cosmic rays in atmospheric aerosol
421 nucleation, *Nature*, 476, 429–433, <https://doi.org/10.1038/nature10343>, 2011.

422 Leng, Q., Cui, J., Zhou, F., Du, K., Zhang, L., Fu, C., Liu, Y., Wang, H., Shi, G., Gao, M., Yang, F., and
423 He, D.: Wet-only deposition of atmospheric inorganic nitrogen and associated isotopic characteristics in
424 a typical mountain area, southwestern China, *Sci. Total Environ.*, 616, 55–63,
425 <https://doi.org/10.1016/j.scitotenv.2017.10.240>, 2018.

426 Li, K., Xu, D., Zhang, L., Liu, W., Zhan, M., Su, Y., Wu, D., and Xie, B.: Integrated isotopic labeling
427 analysis unveils precise proportions of ammonia emissions during composting, *J. Clean. Prod.*, 450,
428 141799, <https://doi.org/10.1016/j.jclepro.2024.141799>, 2024.

429 Li, T., Wang, C., Ji, W., Wang, Z., Shen, W., Feng, Y., and Zhou, M.: Cutting-edge ammonia emissions
430 monitoring technology for sustainable livestock and poultry breeding: a comprehensive review of the
431 state of the art, *J. Clean. Prod.*, 428, 139387, <https://doi.org/10.1016/j.jclepro.2023.139387>, 2023a.

432 Li, T., Li, J., Sun, Z., Jiang, H., Tian, C., and Zhang, G.: High contribution of anthropogenic combustion
433 sources to atmospheric inorganic reactive nitrogen in south China evidenced by isotopes, *Atmospheric
434 Chem. Phys.*, 23, 6395–6407, <https://doi.org/10.5194/acp-23-6395-2023>, 2023b.

435 Lim, S., Lee, M., Czimeczik, C. I., Joo, T., Holden, S., Mouteva, G., Santos, G. M., Xu, X., Walker, J.,
436 Kim, S., Kim, H. S., Kim, S., and Lee, S.: Source signatures from combined isotopic analyses of PM_{2.5}
437 carbonaceous and nitrogen aerosols at the peri-urban taehwa research forest, South Korea in summer and
438 fall, *Sci. Total Environ.*, 655, 1505–1514, <https://doi.org/10.1016/j.scitotenv.2018.11.157>, 2019.

439 Lim, S., Hwang, J., Lee, M., Czimeczik, C. I., Xu, X., and Savarino, J.: Robust evidence of ¹⁴C, ¹³C,
440 and ¹⁵N analyses indicating fossil fuel sources for total carbon and ammonium in fine aerosols in Seoul
441 megacity, *Environ. Sci. Technol.*, 56, 6894–6904, <https://doi.org/10.1021/acs.est.1c03903>, 2022.

442 Liu, M., Huang, X., Song, Y., Tang, J., Cao, J., Zhang, X., Zhang, Q., Wang, S., Xu, T., Kang, L., Cai,

443 X., Zhang, H., Yang, F., Wang, H., Yu, J. Z., Lau, A. K. H., He, L., Huang, X., Duan, L., Ding, A., Xue,
444 L., Gao, J., Liu, B., and Zhu, T.: Ammonia emission control in China would mitigate haze pollution and
445 nitrogen deposition, but worsen acid rain, *Proc. Natl. Acad. Sci.*, 116, 7760–7765,
446 <https://doi.org/10.1073/pnas.1814880116>, 2019.

447 Liu, X., Zhang, Y., Han, W., Tang, A., Shen, J., Cui, Z., Vitousek, P., Erisman, J. W., Goulding, K.,
448 Christie, P., Fangmeier, A., and Zhang, F.: Enhanced nitrogen deposition over China, *Nature*, 494, 459–
449 462, <https://doi.org/10.1038/nature11917>, 2013.

450 Ma, R., Zou, J., Han, Z., Yu, K., Wu, S., Li, Z., Liu, S., Niu, S., Horwath, W. R., and Zhu-Barker, X.:
451 Global soil-derived ammonia emissions from agricultural nitrogen fertilizer application: a refinement
452 based on regional and crop-specific emission factors, *Glob. Change Biol.*, 27, 855–867,
453 <https://doi.org/10.1111/gcb.15437>, 2021.

454 Meng, W., Zhong, Q., Yun, X., Zhu, X., Huang, T., Shen, H., Chen, Y., Chen, H., Zhou, F., Liu, J., Wang,
455 X., Zeng, E. Y., and Tao, S.: Improvement of a global high-resolution ammonia emission inventory for
456 combustion and industrial sources with new data from the residential and transportation sectors, *Environ.*
457 *Sci. Technol.*, 51, 2821–2829, <https://doi.org/10.1021/acs.est.6b03694>, 2017.

458 Pan, Y., Tian, S., Liu, D., Fang, Y., Zhu, X., Gao, M., Wentworth, G. R., Michalski, G., Huang, X., and
459 Wang, Y.: Source apportionment of aerosol ammonium in an ammonia-rich atmosphere: an isotopic study
460 of summer clean and hazy days in urban Beijing, *J. Geophys. Res. Atmospheres*, 123, 5681–5689,
461 <https://doi.org/10.1029/2017JD028095>, 2018.

462 Pan, Y., Gu, M., Song, L., Tian, S., Wu, D., Walters, W. W., Yu, X., Lü, X., Ni, X., Wang, Y., Cao, J., Liu,
463 X., Fang, Y., and Wang, Y.: Systematic low bias of passive samplers in characterizing nitrogen isotopic
464 composition of atmospheric ammonia, *Atmospheric Res.*, 243, 105018–105025,
465 <https://doi.org/10.1016/j.atmosres.2020.105018>, 2020.

466 Qu, Q. and Zhang, K.: Effects of pH, total solids, temperature and storage duration on gas emissions
467 from slurry storage: a systematic review, *Atmosphere*, 12, 1156, <https://doi.org/10.3390/atmos12091156>,
468 2021.

469 Rosa, E., Arriaga, H., and Merino, P.: Ammonia emission from a manure-belt laying hen facility equipped
470 with an external manure drying tunnel, *J. Clean. Prod.*, 251, 119591,
471 <https://doi.org/10.1016/j.jclepro.2019.119591>, 2020.

472 Savard, M. M., Cole, A., Smirnov, A., and Vet, R.: $\delta^{15}\text{N}$ values of atmospheric N species
473 simultaneously collected using sector-based samplers distant from sources – isotopic inheritance and
474 fractionation, *Atmos. Environ.*, 162, 11–22, <https://doi.org/10.1016/j.atmosenv.2017.05.010>, 2017.

475 Schlesinger, William H. and Hartley, Anne E.: A global budget for atmospheric NH_3 , *Biogeochemistry*, 15,
476 <https://doi.org/10.1007/bf00002936>, 1992.

477 Skinner, R., Ineson, P., Jones, H., Sleep, D., and Theobald, M.: Sampling systems for isotope-ratio mass
478 spectrometry of atmospheric ammonia, *Rapid Commun. Mass Spectrom.*, 20, 81–88,
479 <https://doi.org/10.1002/rcm.2279>, 2006.

480 Soler-Jofra, A., Stevens, B., Hoekstra, M., Picioreanu, C., Sorokin, D., Van Loosdrecht, M. C. M., and
481 Pérez, J.: Importance of abiotic hydroxylamine conversion on nitrous oxide emissions during nitrification
482 of reject water, *Chem. Eng. J.*, 287, 720–726, <https://doi.org/10.1016/j.cej.2015.11.073>, 2016.

483 Song, L., Walters, W. W., Pan, Y., Li, Z., Gu, M., Duan, Y., Lü, X., and Fang, Y.: 15N natural abundance
484 of vehicular exhaust ammonia, quantified by active sampling techniques, *Atmos. Environ.*, 255, 118430–
485 118440, <https://doi.org/10.1016/j.atmosenv.2021.118430>, 2021.

486 Song, L., Wang, A., Li, Z., Kang, R., Walters, W. W., Pan, Y., Quan, Z., Huang, S., and Fang, Y.: Large
487 seasonal variation in nitrogen isotopic abundances of ammonia volatilized from a cropland ecosystem
488 and implications for regional NH₃ source partitioning, *Environ. Sci. Technol.*, 58, 1177–1186,
489 <https://doi.org/10.1021/acs.est.3c08800>, 2024.

490 Stratton, J. J., Ham, J., Collett, J. L., Jr., Benedict, K., and Borch, T.: Assessing the efficacy of nitrogen
491 isotopes to distinguish colorado front range ammonia sources affecting rocky mountain national park,
492 *Atmos. Environ.*, 215, <https://doi.org/10.1016/j.atmosenv.2019.116881>, 2019.

493 Streets, D. G., Bond, T. C., Carmichael, G. R., Fernandes, S. D., Fu, Q., He, D., Klimont, Z., Nelson, S.
494 M., Tsai, N. Y., Wang, M. Q., Woo, J.-H., and Yarber, K. F.: An inventory of gaseous and primary aerosol
495 emissions in Asia in the year 2000, *J. Geophys. Res. Atmospheres*, 108,
496 <https://doi.org/10.1029/2002JD003093>, 2003.

497 Sui, Y., Ou, Y., Yan, B., Rousseau, A. N., Fang, Y., Geng, R., Wang, L., and Ye, N.: A dual isotopic
498 framework for identifying nitrate sources in surface runoff in a small agricultural watershed, northeast
499 China, *J. Clean. Prod.*, 246, 119074, <https://doi.org/10.1016/j.jclepro.2019.119074>, 2020.

500 Ti, C., Gao, B., Luo, Y., Wang, X., Wang, S., and Yan, X.: Isotopic characterization of NH_x-N in
501 deposition and major emission sources, *Biogeochemistry*, 138, 85–102, [https://doi.org/10.1007/s10533-](https://doi.org/10.1007/s10533-018-0432-3)
502 018-0432-3, 2018.

503 Ti, C., Xia, L., Chang, S. X., and Yan, X.: Potential for mitigating global agricultural ammonia emission:
504 A meta-analysis, *Environ. Pollut.*, 245, 141–148, <https://doi.org/10.1016/j.envpol.2018.10.124>, 2019.

505 Ti, C., Ma, S., Peng, L., Tao, L., Wang, X., Dong, W., Wang, L., and Yan, X.: Changes of δ¹⁵N values
506 during the volatilization process after applying urea on soil, *Environ. Pollut.*, 270, 116204,
507 <https://doi.org/10.1016/j.envpol.2020.116204>, 2021.

508 Van Damme, M., Clarisse, L., Whitburn, S., Hadji-Lazaro, J., Hurtmans, D., Clerbaux, C., and Coheur,
509 P.-F.: Industrial and agricultural ammonia point sources exposed, *Nature*, 564, 99–103,
510 <https://doi.org/10.1038/s41586-018-0747-1>, 2018.

511 Walters, W. W., Karod, M., Willcocks, E., Baek, B. H., Blum, D. E., and Hastings, M. G.: Quantifying
512 the importance of vehicle ammonia emissions in an urban area of northeastern USA utilizing nitrogen
513 isotopes, *Atmospheric Chem. Phys.*, 22, 13431–13448, <https://doi.org/10.5194/acp-22-13431-2022>,
514 2022.

515 Wang, C., Yin, S., Bai, L., Zhang, X., Gu, X., Zhang, H., Lu, Q., and Zhang, R.: High-resolution ammonia

516 emission inventories with comprehensive analysis and evaluation in henan, china, 2006–2016, *Atmos.*
517 *Environ.*, 193, 11–23, <https://doi.org/10.1016/j.atmosenv.2018.08.063>, 2018.

518 Wang, C., Li, X., Zhang, T., Tang, A., Cui, M., Liu, X., Ma, X., Zhang, Y., Liu, X., and Zheng, M.:
519 Developing nitrogen isotopic source profiles of atmospheric ammonia for source apportionment of
520 ammonia in urban beijing, *Front. Environ. Sci.*, 10, <https://doi.org/10.3389/fenvs.2022.903013>, 2022.

521 Warner, J. X., Dickerson, R. R., Wei, Z., Strow, L. L., Wang, Y., and Liang, Q.: Increased atmospheric
522 ammonia over the world's major agricultural areas detected from space, *Geophys. Res. Lett.*, 44, 2875–
523 2884, <https://doi.org/10.1002/2016gl072305>, 2017.

524 Wu, L., Ren, H., Wang, P., Chen, J., Fang, Y., Hu, W., Ren, L., Deng, J., Song, Y., Li, J., Sun, Y., Wang,
525 Z., Liu, C.-Q., Ying, Q., and Fu, P.: Aerosol ammonium in the urban boundary layer in beijing: insights
526 from nitrogen isotope ratios and simulations in summer 2015, *Environ. Sci. Technol. Lett.*, 6, 389–395,
527 <https://doi.org/10.1021/acs.estlett.9b00328>, 2019.

528 Wu, L., Zhang, Y., Xiao, Y., Zhu, J., Shi, Z., Wang, Y., Xu, H., Hu, W., Deng, J., Tang, M., and Fu, P.:
529 Diversity of ammonia sources in tianjin: nitrogen isotope analyses and simulations of aerosol ammonium,
530 *Environ. Chem.* 14482517, 21, 1–13, <https://doi.org/10.1071/EN24030>, 2024.

531 Xi, D., Xiao, Y., Mgelwa, A. S., and Kuang, Y.: Formation pathways and source apportionments of
532 inorganic nitrogen-containing aerosols in urban environment: insights from nitrogen and oxygen isotopic
533 compositions in guangzhou, china, *Atmos. Environ.*, 309,
534 <https://doi.org/10.1016/j.atmosenv.2023.119888>, 2023.

535 Xiang, Y.-K., Dao, X., Gao, M., Lin, Y.-C., Cao, F., Yang, X.-Y., and Zhang, Y.-L.: Nitrogen isotope
536 characteristics and source apportionment of atmospheric ammonium in urban cities during a haze event
537 in northern China plain, *Atmos. Environ.*, 269, 118800–118813,
538 <https://doi.org/10.1016/j.atmosenv.2021.118800>, 2022.

539 Xiao, H., Ding, S.-Y., Ji, C.-W., Li, Q.-K., and Li, X.-D.: Combustion related ammonia promotes PM2.5
540 accumulation in autumn in tianjin, china, *Atmospheric Res.*, 275,
541 <https://doi.org/10.1016/j.atmosres.2022.106225>, 2022.

542 Xiao, H., Xiao, H.-W., Xu, Y., Zheng, N.-J., and Xiao, H.-Y.: Combustion-driven inorganic nitrogen in
543 PM2.5 from a city in central china has the potential to enhance the nitrogen load of north China, *J. Hazard.*
544 *Mater.*, 483, <https://doi.org/10.1016/j.jhazmat.2024.136620>, 2025.

545 Xiao, H.-W., Wu, J.-F., Luo, L., Liu, C., Xie, Y.-J., and Xiao, H.-Y.: Enhanced biomass burning as a
546 source of aerosol ammonium over cities in central China in autumn, *Environ. Pollut.*, 266, 115278,
547 <https://doi.org/10.1016/j.envpol.2020.115278>, 2020.

548 Xie, Y., Xiong, Z., Xing, G., Yan, X., Shi, S., Sun, G., and Zhu, Z.: Source of nitrogen in wet deposition
549 to a rice agroecosystem at tai lake region, *Atmos. Environ.*, 42, 5182–5192,
550 <https://doi.org/10.1016/j.atmosenv.2008.03.008>, 2008.

551 Xu, P., Li, G., Zheng, Y., Fung, J. C. H., Chen, A., Zeng, Z., Shen, H., Hu, M., Mao, J., Zheng, Y., Cui,

552 X., Guo, Z., Chen, Y., Feng, L., He, S., Zhang, X., Lau, A. K. H., Tao, S., and Houlton, B. Z.: Fertilizer
553 management for global ammonia emission reduction, *Nature*, 626, 792–798,
554 <https://doi.org/10.1038/s41586-024-07020-z>, 2024.

555 Yang, F., Tan, J., Zhao, Q., Du, Z., He, K., Ma, Y., Duan, F., Chen, G., and Zhao, Q.: Characteristics of
556 PM_{2.5} speciation in representative megacities and across china, *Atmospheric Chem. Phys.*, 11, 5207–
557 5219, <https://doi.org/10.5194/acp-11-5207-2011>, 2011.

558 Zhang, H., Hong, Z., Wei, L., Thornton, B., Hong, Y., Chen, J., and Zhang, X.: Stable isotopes unravel
559 the sources and transport of PM_{2.5} in the Yangtze River delta, china, *Atmosphere*, 14,
560 <https://doi.org/10.3390/atmos14071120>, 2023.

561 Zhang, L., Altabet, M. A., Wu, T., and Hadas, O.: Sensitive measurement of NH₄⁺ 15N/14N ($\delta^{15}\text{NH}_4^+$) at
562 natural abundance levels in fresh and saltwaters, *Anal. Chem.*, 79, 5297–5303,
563 <https://doi.org/10.1021/ac070106d>, 2007.

564 Zhou, Y., Zheng, N., Luo, L., Zhao, J., Qu, L., Guan, H., Xiao, H., Zhang, Z., Tian, J., and Xiao, H.:
565 Biomass burning related ammonia emissions promoted a self-amplifying loop in the urban environment
566 in kunming (SW china), *Atmos. Environ.*, 253, <https://doi.org/10.1016/j.atmosenv.2020.118138>, 2021.

567 Zou, D., Sun, Q., Liu, J., Xu, C., and Song, S.: Seasonal source analysis of nitrogen and carbon aerosols
568 of PM_{2.5} in typical cities of zhejiang, china, *Chemosphere*, 303,
569 <https://doi.org/10.1016/j.chemosphere.2022.135026>, 2022.

570